# Sinusoidal phase modulating laser diode interferometer using an additive operating type of integrating bucket method

Xuefeng Zhao, Takamasa Suzuki*, Osami Sasaki
Faculty of Engineering, Niigata University, Japan

## ABSTRACT

We propose a sinusoidal phase modulating laser diode interferometer using an additive operating type of integrating bucket method. In previous integrating bucket method, four images, which are integrated values of the interference pattern detected by a CCD image sensor, are required. According to additive and subtractive operations in a calculator, the quadrature signals can be calculated from these images. While these operations are associated with the technical computing software, such as MATLAB, in a personal computer, it is quite fast, even if the images possess large size. In a standard-alone system with a CPU, however, this kind of operation expends unbearable time. To lighten the burden of the calculator, we tried to simplify the operation. That is, on the basis of integrating bucket method, the subtraction in the signal processing is transformed to the addition by use of the phase shifting technique. All additive operations are achieved with the CCD image sensor. In this interferometer, not only the calculating quantity is reduced, but also the number of required images is reduced. The surface profile of a diamond-turned aluminum disk was measured. The repeatability in the measurements was 5.93 nm rms.

Keywords: sinusoidal phase modulation, laser diode, interferometer, integrating bucket method

## 1. INTRODUCTION

As an important phase analyzing method, the integrating bucket method[1], which is used in the sinusoidal phase modulating interferometer (SPM)[2], has the advantage of high speed, high accuracy, and simple construction and it is wildly used for such applications as measurements of surface profile, lengths, and displacement, etc. In a SPM interferometer using this method, four integrated values of the interference pattern are required. The quadrature signals in which the phase information of the object's surface profile is contained can be calculated by using addition and subtraction operating from them. Normally, we employ a CCD image sensor[3] to integrate the interference patterns. In recent years, as technology progresses, the CCD has had remarkable improvements. Even through a low cost simpler CCD camera, the surface of an object can be measured with high-resolution and large size. However, accompanied by the increasing of the pixel numbers of images, the data volume that needs to be processed is greatly increased. Therefore, it is required that the data processing system has high performance. MATLAB is typical technical computing software. It is famous for the high-speed matrix operation. Coupled with MATLAB, even a personal computer enables us to process large size images quickly, according to the integrating bucket method. But, unfortunately, the software design in a stand-alone system is not to be compared with MATLAB for data processing. Even though the operating speed of the system's calculator is quite quick, it may still take unbearable time when the images possess large size are being processed. To lighten the burden of these kinds of data processing system, we tried to simplify the operation. That is, on the basis of integrating bucket method, the subtractive operating in the signal processing is transformed to the additive operating by use of the phase shifting technique. All additive operations are achieved with the CCD image sensor. In this paper, we expound the principle of this efficient integrating bucket method and the construction of a SPM interferometer using this method. In experiment, a diamond-turned aluminum disk was measured with this interferometer.

## 2. PRINCIPLE

### 2.1 SPM interferometry

One of the characteristics of the laser diode (LD) is that its wavelength varied with the injection current or the

Advanced Materials and Devices for Sensing and Imaging, Jianquan Yao, Yukihiro Ishii,
Editors, Proceedings of SPIE Vol. 4919 (2002) © 2002 SPIE · 0277-786X/02/$15.00

temperature. We call them current modulation[4] and thermal modulation[5]. Take current modulation for example, when a variable current $\Delta I$ is injected into a LD, the interference signal of a Twyman-Green interferometer is

$$S(t) = S_1(t) + S_0(t)\cos(\Delta\phi + \alpha), \tag{1}$$

where

$$\Delta\phi = \frac{4\pi l}{\lambda_0^2}\beta\Delta I, \tag{2}$$

and

$$\alpha = \frac{4\pi l}{\lambda_0} \tag{3}$$

are phase change of the interference signal caused by current modulation and initial phase that depends on the optical path difference (OPD), respectively. $S_1(t), S_0(t)$, $\lambda_0$, $2l$ and $\beta$ are dc component of the interference signal, ac component of the interference signal, wavelength of the LD, OPD and efficiency of the current modulation, respectively. Furthermore when a sinusoidal current

$$I_m(t) = a\cos(\omega_c t + \theta) \tag{4}$$

is injected into the LD, we can get an SPM interferometer, the interference signal can be given as

$$S(t) = S_1(t) + S_0(t)\cos[z\cos(\omega_c t + \theta) + \alpha], \tag{5}$$

where $z = \frac{4\pi a\beta l}{\lambda_0^2}$ is the modulation depth.

### 2.2 Integrating bucket method

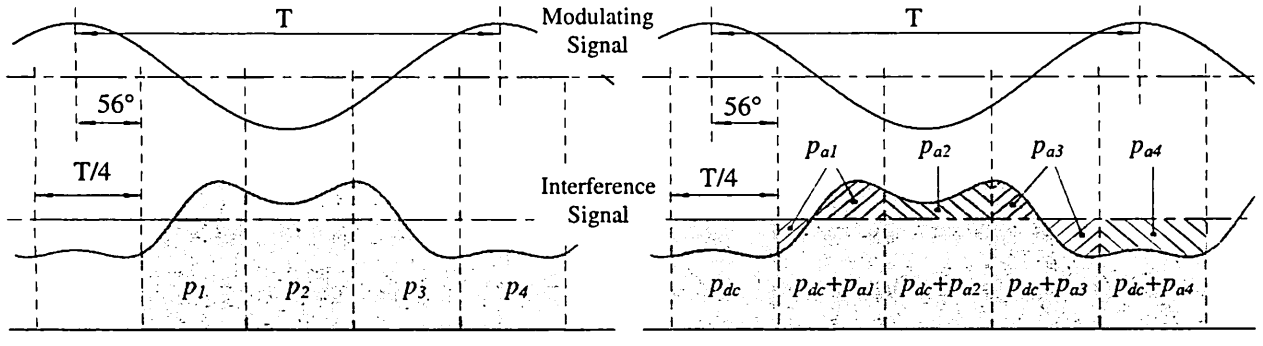


(a) (b)

Figure 1 Integrating bucket method

The phase difference $\alpha$ in the SPM interferometer can be obtained with the integrating bucket method. It's principle is shown in Fig. 1.(a). The interference signal is sequentially integrated four times in a modulation period with the integrating time of a quarter modulation period. Normally, we use a CCD image sensor to integrate interference signal and four integrated values $p_1$~$p_4$ can be obtained as images. From these images, two quadrature values can be calculated as

$$\begin{aligned} p_s &= p_1 + p_2 - p_3 - p_4 \\ &= A_s \sin\alpha \end{aligned} \tag{6}$$

and

$$\begin{aligned} p_c &= p_1 - p_2 + p_3 - p_4 \\ &= A_c \cos\alpha \end{aligned} \tag{7}$$

In which, $A_s$ and $A_c$ are the functions of both modulation depth $z$ and initial phase $\theta$ of the modulating current. When $z = 2.45$ and $\theta = 56°$, $A_s = A_c$ can be achieved and the measurement error caused by the noise becomes minimum[1]. The phase $\alpha$ can then be given by

$$\alpha = \tan^{-1}\left(\frac{p_s}{A_s} / \frac{p_c}{A_c}\right)$$

$$\Downarrow \quad z=2.45 \ \& \ \theta=56°$$

$$\alpha = \tan^{-1}\left(\frac{p_s}{p_c}\right) = \tan^{-1}\left(\frac{p_1 + p_2 - p_3 - p_4}{p_1 - p_2 + p_3 - p_4}\right) \tag{8}$$

### 2.3 Additive operating type of integrating bucket method

According to the principle of the integrating bucket method mentioned above, to get the quadrature signals $p_s$ and $p_c$, we must integrate interference pattern four times with a CCD and capture them as the images first. Then two times additive operations and four times subtractive operations need to be done in a calculator. At present there are tens thousand or millions pixels in a CCD image sensor, even in a low cost simpler one. That is to say, a great quantity of data, which are six times the numbers of pixel, need to be processed if the integrating bucket method is used. MATLAB, the language of technical computing, is famous in the matrix processing. A normal PC, together with MATLAB, can process this kind of operation without difficulty. But it is a great burden for a stand-alone system. For the low capacity of the data processor in the stand-alone system and there is no software designed for it can be compared to MATLAB in a PC. To reduce the data volume that need to be processed, we propose an efficient additive operating type of integrating bucket method.

As is known to all, the charge coupled device or CCD image sensor is a photo detector which can integrate the intensity of the light upon it and transmit the result as video signal. Consequently, the additive operating of a number of integrated values can be realized on the CCD. On the basis of this characteristic, we try to let parts of operation achieve on the CCD but not in the calculator.

As shown in Fig. 1.(b), we express the integrated values as the sum of dc component and ac component:

$$p_i = p_{dc} + p_{ai} \quad (i = 1 \sim 4) . \tag{9}$$

Then the Eq. (6) and Eq. (7) can be rewritten as

$$\begin{aligned} p_s &= (p_{dc} + p_{a1}) + (p_{dc} + p_{a2}) - (p_{dc} + p_{a3}) - (p_{dc} + p_{a4}) \\ &= p_{a1} + p_{a2} - p_{a3} - p_{a4} \end{aligned} , \tag{10}$$

and

$$\begin{aligned} p_s &= (p_{dc} + p_{a1}) - (p_{dc} + p_{a2}) + (p_{dc} + p_{a3}) - (p_{dc} + p_{a4}) \\ &= p_{a1} - p_{a2} + p_{a3} - p_{a4} \end{aligned} , \tag{11}$$

respectively.

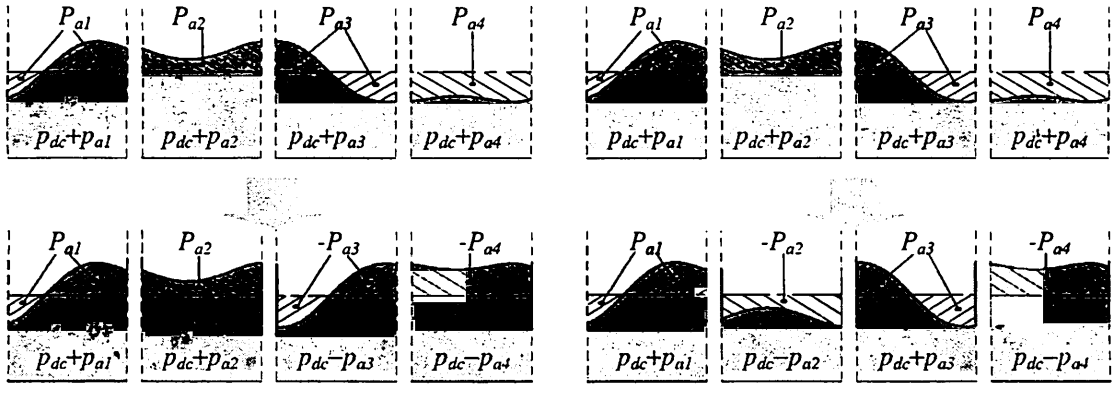


(a) (b)

Figure 2 Changing the sign of the interference signal's ac component

In order to enable the additive operation on the CCD, we try to change the sign of the interference signal's ac component. The method is shown in Fig. 2. In Fig. 2.(a), the signs of $p_{a1}$ and $p_{a2}$ are kept and the signs of $p_{a3}$ and $p_{a4}$ are

inversed. Then, the sum of the integrated values is given by

$$\begin{aligned} P_s &= (p_{dc} + p_{a1}) + (p_{dc} + p_{a2}) + (p_{dc} - p_{a3}) + (p_{dc} - p_{a4}) \\ &= p_s + 4p_{dc} \end{aligned} \quad (12)$$

Similar with Fig. 2.(a), the signs of $p_{a1}$ and $p_{a3}$ are kept and the signs of $p_{a2}$ and $p_{a4}$ are inversed as shown in Fig. 2.(b). We can obtain

$$\begin{aligned} P_c &= (p_{dc} + p_{a1}) + (p_{dc} - p_{a2}) + (p_{dc} + p_{a3}) + (p_{dc} - p_{a4}) \\ &= p_c + 4p_{dc} \end{aligned} \quad (13)$$

Since $P_s$, $P_c$ and additional terms $4p_{dc}$ are all the sum of the integrated values, it is possible to sequentially integrate them on the CCD in three modulation periods. Then, $p_s = P_s - 4p_{dc}$ and $p_c = P_c - 4p_{dc}$ are processed in the calculator and the number of the operations is reduced to only two times. That is to say, the amount of calculation decreased by 2/3 and the burden of the calculator can be greatly lightened especially in a stand-alone system.

As pointed out above, the main aspect in the additive type of integrating bucket method is: in the light of previous integrating bucket method, change the subtractive operation to additive operation and fit for operation on the CCD. Now the problem is how to realize the sign inversion. For this end, we analyze the interference signal in current modulation again. The interference signal expressed in Eq. (5) corresponds to the sinusoidal modulating current $I_m(t) = a\cos(\omega_c t + \theta)$. If an additional dc bias current $\Delta I_{dc}$ is added into $I_m(t)$ or the current

$$I_m(t) = a\cos(\omega_c t + \theta) + \Delta I_{dc} \quad (14)$$

is injected into the LD, the interference signal can be given as

$$S(t) = S_1(t) + S_0(t)\cos[z\cos(\omega_c t + \theta) + \alpha + \Delta\phi]. \quad (15)$$

Where $\Delta\phi$ is the phase shift corresponding to the $\Delta I_{dc}$. If it is set to $\pi$ by adjusting $\Delta I_{dc}$, the ac component's sign of the interference signal is inversed:

$$\begin{aligned} S(t) &= S_1(t) + S_0(t)\cos[z\cos(\omega_c t + \theta) + \alpha + \pi] \\ &= S_1(t) - S_0(t)\cos[z\cos(\omega_c t + \theta) + \alpha] \end{aligned} \quad (16)$$

Substituting $\Delta\phi = \pi$ into Eq. (2), the value of $\Delta I_{dc}$ can be find as

$$\Delta I_{dc} = \frac{\Delta\phi\lambda_0^2}{4\pi l\beta} = \frac{\pi\lambda_0^2}{4\pi l\beta} = \frac{\pi}{z}a. \quad (17)$$

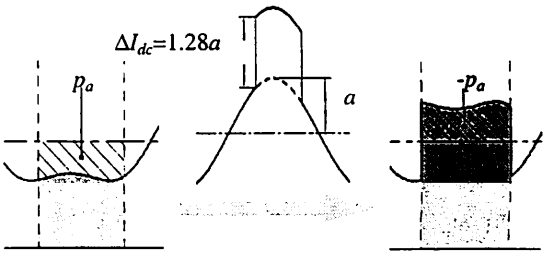


Figure 3 Schematic of the sign inversion

Make use of the condition $z$ = 2.45 in the integrating bucket method, we can know when a additional dc bias current $\Delta I_{dc} = 1.28a$ is injected into the LD as shown in Fig. 3, the phase of the interference signal is shifted by $\pi$ and the inversion of the ac component's sign of the interference signal can be realized.

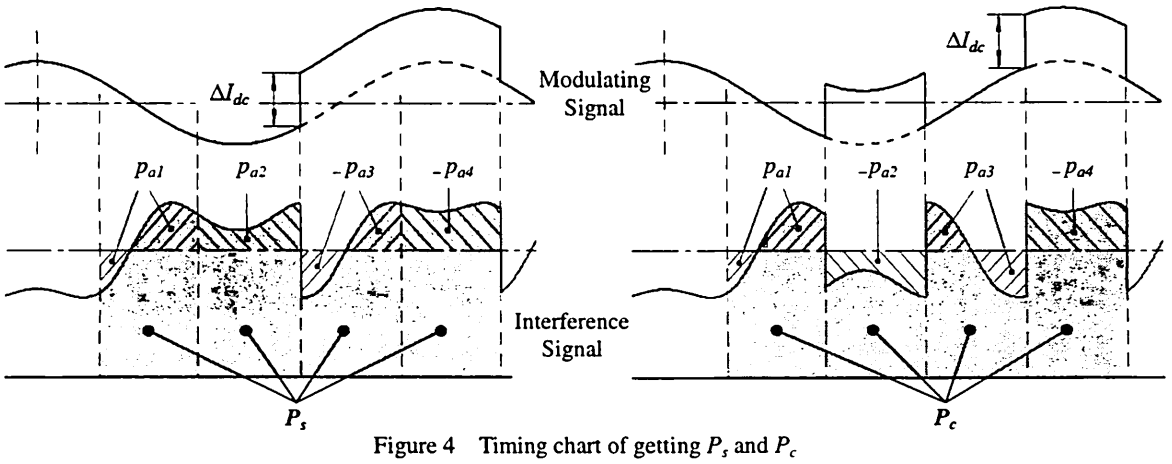


Figure 4 Timing chart of getting $P_s$ and $P_c$

We may summarize our arguments as follows. In two integrating periods, as long as the modulating currents shown in Fig. 4 are injected into the LD, the $P_s$ and $P_c$ can be integrated on the CCD.

To calculate $p_s$, and $p_c$, $4p_{dc}$ has yet to be eliminated from $P_s$ and $P_c$. Next we discuss how to realize it.

Eq. (15) can be rewrite as

$$S(t) = S_1(t) + S_0(t)\cos[\alpha + \Delta\phi(t)], \qquad (18)$$

where we presume the amplitude of the sinusoidal signal is set to zero and $\Delta\phi$ is a temporary variable. According to the integrating characteristic of the cosine function, when the phase $\Delta\phi$ is linearly changed $2\pi$, the integrated result of the AC component in Eq. (18) is zero. So we linearly change $\Delta\phi$ from $-\pi$ to $\pi$ in a modulating period as shown in Fig. 5, and $4p_{dc}$ can be integrated on the CCD. Substituting $\Delta\phi = 2\pi$ into Eq. (2), we can find the amplitude of the linear change as $2.56a$.

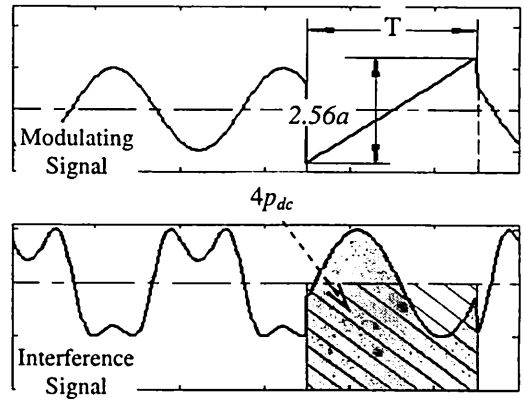


Figure 5 Getting $4p_{dc}$ through linear changing the modulating current

To improve the performance of the feedback control system and eliminate the external disturbance effectively, we proposed a new method that can increase the modulating speed with a normal CCD camera provided with shutter function[6, 7]. Fig. 6.(a) shows the timing chart when it is used in a SPM interferometer using integrating bucket method. After the integrating time is shortened by using the shutter function, limited by the NTSC system, four integrated values $p_1$~$p_4$ cannot but be obtained in four sequential frame time. And a quarter modulating period should be adjusted carefully to fit the shutter speed and shifted $\pi/2$ in next frame time.

In present experiment, we use the normal CCD camera to integrate the interference pattern as well. The timing chart is shown in Fig. 6. (b). Different with the method shown in Fig. 6.(a), the modulating period is set to same with the shutter speed of the CCD camera and the initial phase of the modulating signal in different integrating time is kept constant. After the modulating current as shown in Fig. 6.(b) is injected into the LD, the CCD camera output $P_s$, $P_c$ and $4p_{dc}$ as video signals in three frame time. Because the required image numbers are reduced from four to three, in present method, the measurement time is reduced as well. It is obvious in the using of a normal CCD camera, for the integrated values are outputted at intervals of one frame time in the NTSC system.

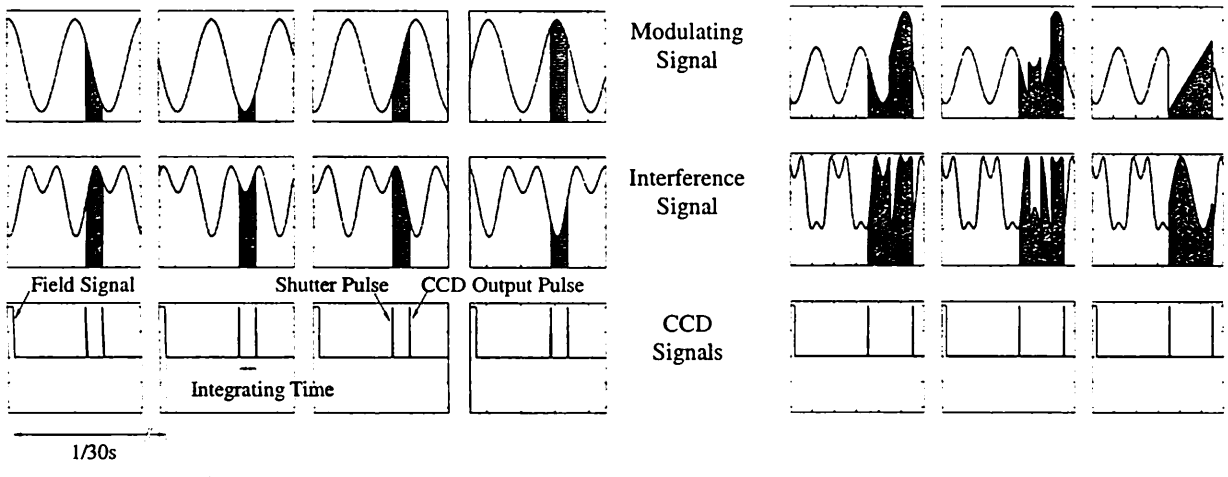


(a) Previous integrating bucket method (b) Present integrating bucket method

Figure 6 Timing chart using a normal CCD camera provided with shutter function

## 3. EXPERIMENTS

The experimental setup is diagramed in Fig. 7. The optical source of the Twyman-Green type interferometer is a laser diode (Mitsubishi ML1412R) whose wavelength is 685nm and output power is 30mW. The interferometer is constructed with a reference mirror, an object and a beam splitter (BS1). The OPD is 50mm. A parts of laser beam pass through the BS2 and interfere on the CCD (Sony ICX058CL) whose pixel numbers are 768(H)×494(V) with a

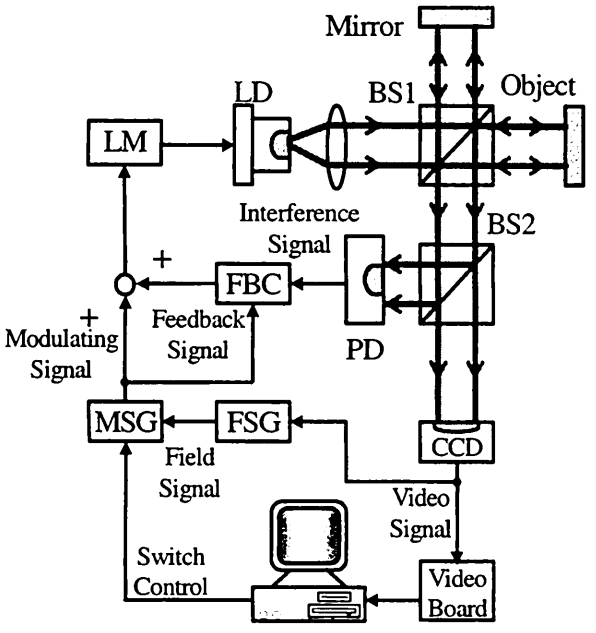


LD: Leaser Diode LM: Leaser Modulator
BS: Beam Splitter FBC: Feedback Control
FSG: Field Signal Generator
MSG: Modulating Signal Generator

Figure 7 Experimental setup

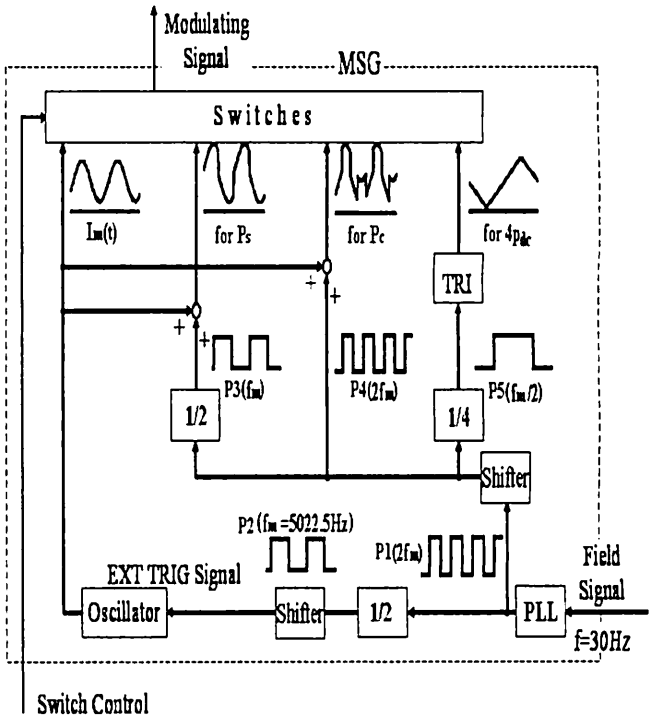


Figure 8 Block diagram of the MSG

unit cell size of 6.35μm(H)×7.40μm(V). The CCD camera integrates the interference pattern and outputs the result as the video signal. Using a video capture board, the images are captured with the size of 320×240 pixels.

The modulating signal is generated with a modulating signal generator (MSG) as shown in Fig. 8. The source signal is the field signal separated from the video signal by using a field signal generator (FSG). Through a phase-locked loop (PLL), a pulse P1 whose frequency is two times that of modulating signal is generated. Passing this pulse through a 1/2 frequency divider and a phase shifter, then inject it into the oscillator as an external source, the sinusoidal modulating signal with an amplitude $a$ and an initial phase $\theta = 56°$ is synchronously generated. Mixing this modulating signal with two pulses P3 and P4, whose frequency are half and same with the P1 and the amplitudes are all $1.28a$, the modulating signal for getting $P_s$ and $P_c$ can be generated as well. The modulating signal for generating $4p_{dc}$ is a triangle pulse whose amplitude is $2.56a$. It is generated from the pulse P1 with a 1/4 frequency divider and a triangle pulse generator. The selection of these four forms of modulating signal is controlled by the computer and we finally can obtain the modulating signals as shown in Fig. 6.(b).

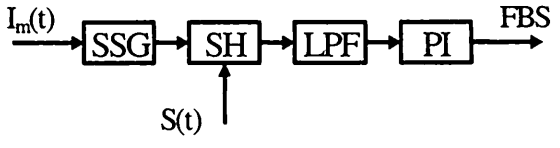


$I_m(t)$: Modulating Signal S(t): Interference Signal
FBS: Feedback Signal LPF: Low-Pass Filter
SH: Sample Hold SSG: Sampling Signal Generator
PI: Proportional and Integral controller

Figure 9 Block diagram of the FBC

In experiment, the shutter speed of the CCD camera is set to 1/5000. According to the actual integrating time of 199μs, the frequency of the sinusoidal modulating signal is set to 5022.5Hz. Because the dc component of the interference signal is added four times and it may reduce the experiment accuracy, extreme care must be exercised to increase the visibility of the interference signal as much as possible.

On the other hand, another parts of the leaser beam are reflected by the BS2 and interfere on the photo detector (PD). The interference signal detected by the PD is injected into the feedback controller (FBC). Fig. 9 shows the block diagram of the FBC. In the FBC, the pulse signal synchronized with the modulating signal is generated in the SSG and samples the interference signal in the sample-hold circuit (SH). Then the output signal is smoothed by a low pass filter

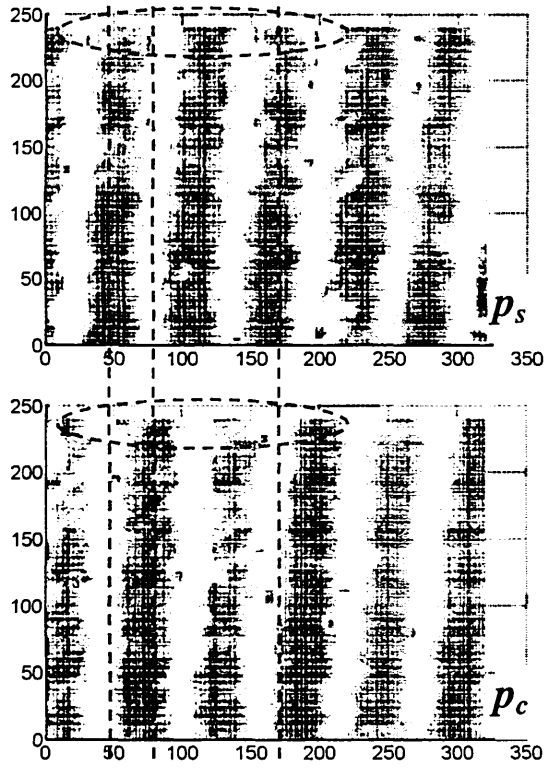


Figure 10 Calculated two-dimensional $p_s$ and $p_c$

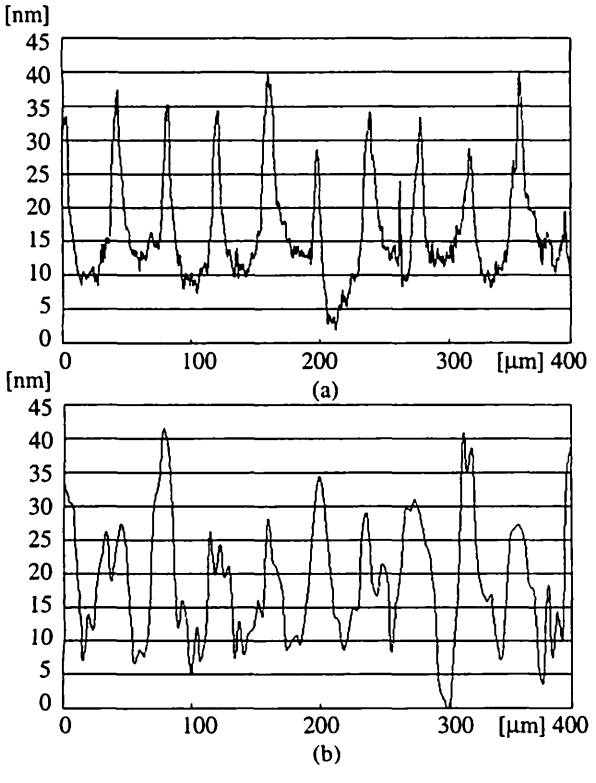


Figure 12 Two-dimensional surface profiles of a diamond-turned aluminum disk

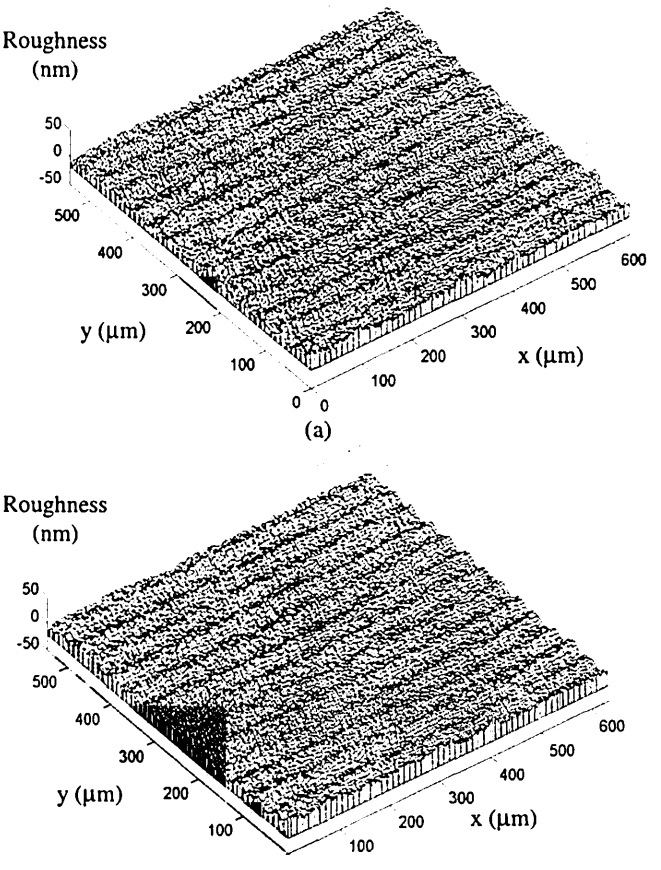


(b) After ten minutes

Figure 11 Three-dimensional surface profiles of a diamond-turned aluminum disk

(LPF) whose cut-off frequency is 120Hz. After passing a proportional and integral controller (PI), the feedback signal is finally obtained. Base on the phase-locked technology[8], the phase of the interference signal is locked and the external disturbance is eliminated.

## 4. RESULT

We used a diamond-turned aluminum disk as a measurement object. We first tilted the object and captured the images of $P_s$, $P_c$ and $4p_{dc}$. The calculated $p_s = P_s - 4p_{dc}$ and $p_c = P_c - 4p_{dc}$ are shown as two-dimensional images in Fig. 10. The dashed lines indicate that the phase difference between $p_s$ and $p_c$ is $\pi/2$. It is consistent with the theory.

Fig. 11 shows the three-dimensional surface profiles of the aluminum disk. The ditch shape cut by the diamond is clearly discernable. The two-dimension surface profiles measured with (a): Taly-step profilometer and (b): our system are

shown in Fig. 12. Although the measured positions are different, the roughness and the cutting pitch are in good agreement. The same position was measured several times at intervals of ten minutes and we obtained the repeatability of 5.93nm rms.

## 4. CONCLUTION

We proposed a sinusoidal phase modulating laser diode interferometer using an additive operating type of integrating bucket method. In this method, some calculating operations that need to be done in the calculator in previous method were changed to execute on the CCD. The burden of the calculator, especially in the stand-alone system, was lightened. At the same time, for the required image numbers are reduced, the measurement time is also reduced. Using this measurement system, we measured the object and get a repeatability of 5.93nm rms.

## REFERENCES

1. O. Sasaki, H. Okazaki and M. Sakai, "Sinusoidal phase modulating interferometer using the integrating-bucket method," Appl. Opt. 26, pp. 1089-1093, 1987.
2. O. Sasaki and H. Okazaki, "Sinusoidal phase modulating interferometry for surface profile measurement," Appl. Opt. 25, pp. 3137-3140, 1986.
3. O. Sasaki and H. Okazaki, "Detection of time-varying intensity distribution with CCD image sensor," Appl. Opt. 24, pp. 2124-2126, 1985.
4. K. Tatsuno and Y. Tsunoda, "Diode laser direct modulation heterodyne interferometer," Appl. Opt. 26, pp. 37-40, 1987.
5. T. Suzuki, M. Matsuda, O. sasaki and T. Maruyama, "Laser-diode interferometer with a photothermal modulation" Appl. Opt. 38, pp. 7069-7075, 1999.
6. X. Zhao, T. Suzuki and O. Sasaki, "Photo-thermal phase-modulating laser diode interferometer with high-speed feedback control," Opt. Rev. 9, pp. 13-17, 2002.
7. T. Suzuki, T. Maki, X. Zhao, and O. Sasaki, "Disturbance-free high-speed sinusoidal phase-modulating laser diode interferometer," Appl. Opt. 41, pp. 1949-1953, 2002.
8. T. Suzuki, O. sasaki and T. Maruyama, "Phase locked laser diode interferometry for surface profile measurement" Appl. Opt. 28, pp. 4407-4410, 1989 .

*Correspondence: takamasa@eng.niigata-u.ac.jp; phone:+81-25-262-7215; fax:+81-25-262-7215; http://teoptlab.eng.niigata-u.ac.jp; Faculty of Engineering, Niigata University, 8050 Ikarashi 2, Japan 950-2181